Answer to the 1st ATAC Report

Including Vibration and Error Analysis

Linac summary: study and development

2nd ATAC Meeting for J-PARC Project

2003.3.7

KEK T. Kato

Subjects requested by ATAC2002 committee

- Investigation of the pulse-to-pulse energy variation.
- Progress of the vibration and error analysis.
- The effect of the tapered gradient of the ACS for dedicated matching.
- Estimation of the halo generated from the chopper transit, and the solution to avoid the partially kicked beam through the linac.
- End-to-end multi-particle simulation.
- L3BT modification

Linac design and operation (basic idea)

- Tunable operation is necessary
  - Against peak-current variation
  - Against errors: Machine, Beam, Tuning
- Variable and sufficient focusing strength
  - Against strong space-charge effects
- Tuning of the transition part
  - Achieve matched injection
  - Adjust accumulate errors before

MEBT2 between SDTL and ACS

- **Variable matching section between the SDTL and the ACS is an important knob for matching and tuning**
  - **Longitudinal transition with three times the frequency**
  - **Transverse transition with a small change in focusing length**

Therefore, a fixed configuration (tapered gradient of the ACS) is not adopted

MEBT design (from RFQ to DTL)

Three purposes:

- Beam matching
- Beam chopping
  - Some space for the deflecting chopped beam is indispensable for obtaining sufficient separation
  - Chopping
    - it costs some emittance growth along the MEBT
      - » <u>**If it is allowable, the MEBT is totally acceptable**</u>
- Beam measurement

Static and random errors

- Static errors
  - Compensation is possible
- Random errors (pulse to pulse or within pulse)
  - No effective compensation method

1. Eliminate or suppress random errors from the linac system
2. minimize static errors

   ---> suppress mode mixing

   ---> construct all components with sufficient accuracy
3. Use tunable and sufficient focusing systems

Achieved stability or accuracy (static)

Achieved results:

- **DTL field distribution ~ ± 1%**
- **DTL Q-magnet center alignment**
  - **~within ± 50 μm**
- **RF structure alignment accuracy ~ ± 50 ~ 100 μm**
  - **According to the preliminary laser experiments**
- **Water temperature control ~ ± 0.1-0.2 degrees (design)**

Achieved pulse-to-pulse stability (random)

- **RF amplitude and phase variation**
  - **Amplitude < ± 0.3%, phase < ± 0.3 degrees**
- **Vibration of drift tube due to water flow and pulsed Q-magnet excitation**
  - **Water flow**
    - Negligibly small
  - **Pulse Q-mag. Excitation (1000 A, 50 Hz)**
    - **~ 1.5 μm**
  - **Simulation is not necessary since the displacement is very small**

Tuning of the DTL-1 field

(Naito)

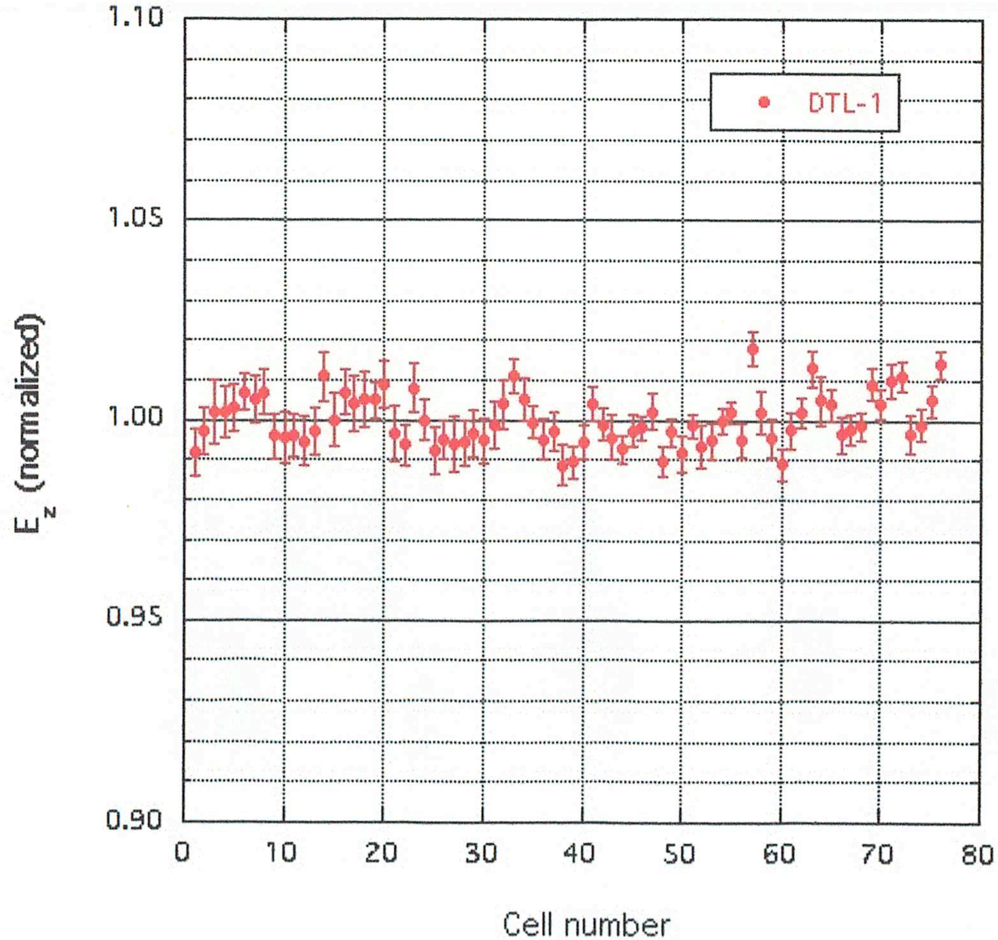

Field distribution
0.989 - 1.018
Accuracy ±0.005

DTL-1
76 cells
9.9 m

Measurements and alignment of DTQ

(Naito)

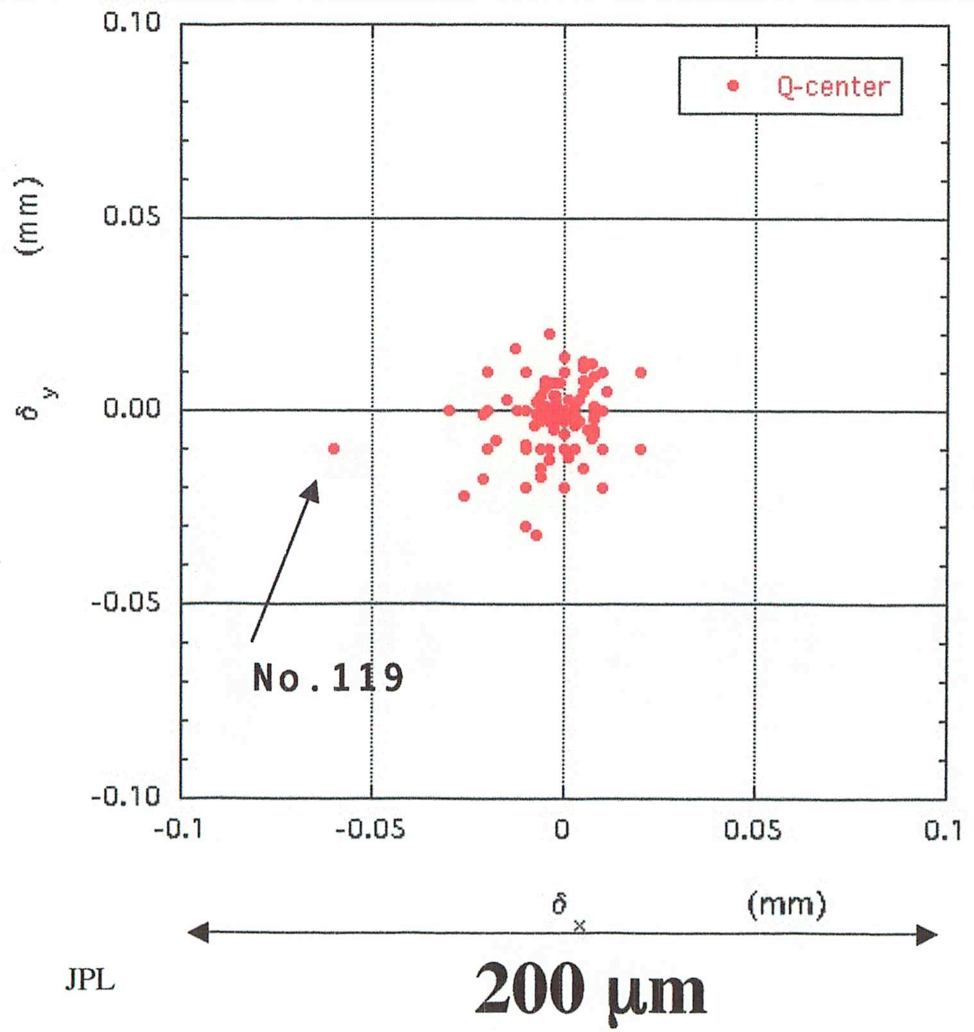

Deviation of the Q-mag center from mechanical center

x -30 ~ +20 μm

y -32 ~ +20 μm

After installing into DT

x -50 ~ +50 μm

y -40 ~ +40 μm

Note: Adjust the offset of No.119 in the installation into DT.

RF field stability (Yamaguchi)

experimental results during MEBT beam study

Required field stability has been achieved by using analog feedback method.

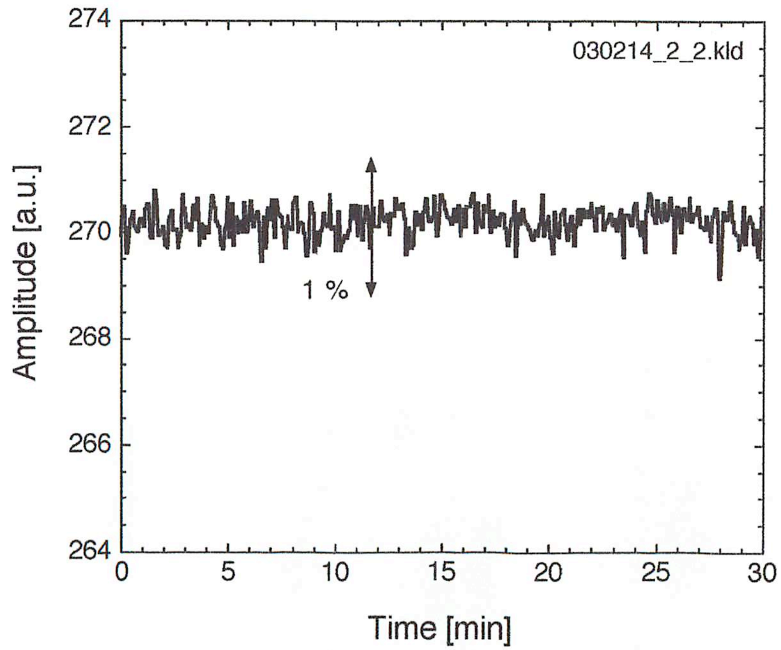

RFQ tank amplitude
29 mA beam

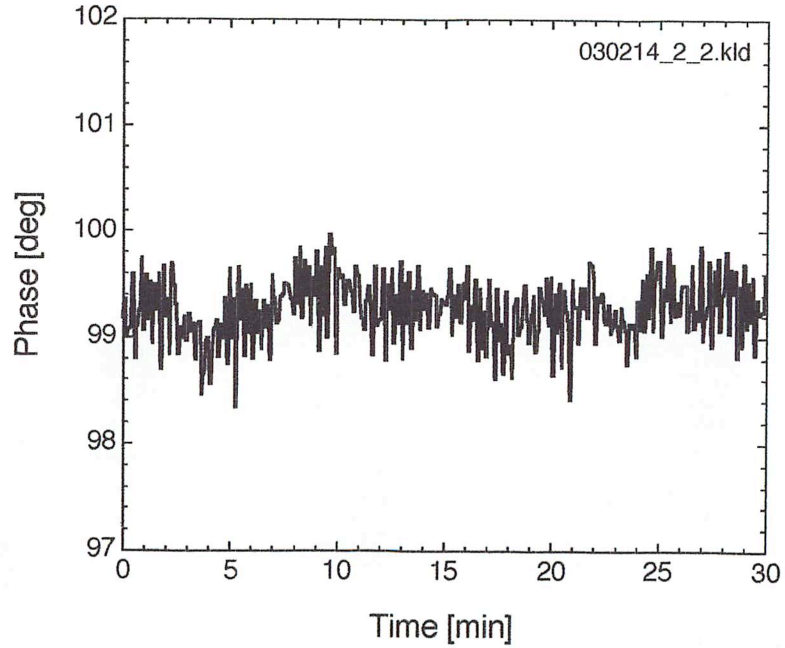

RFQ tank phase
29 mA beam

RF field stability (Michizono)

experimental results of SDTL tank

Digital feedback method

I/Q measurement

±0.4%

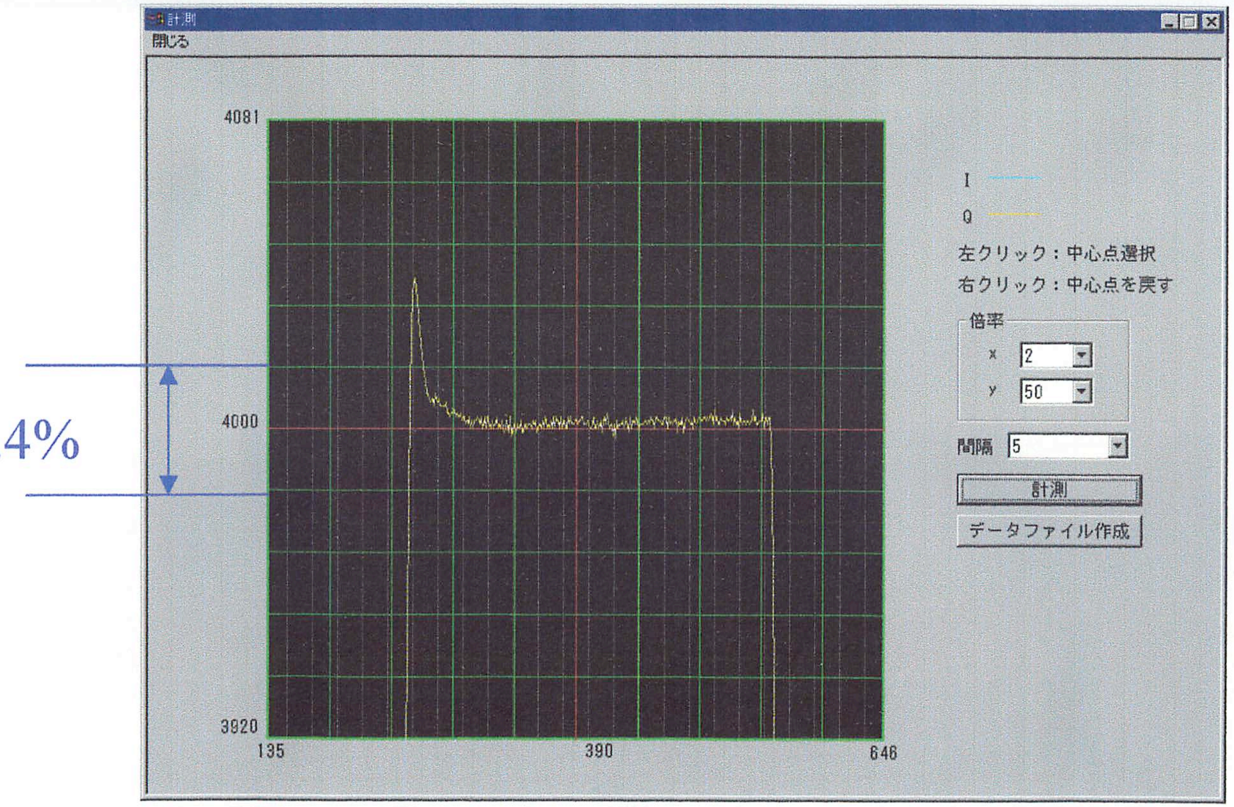

✧ Stability:~±0.2%

Accuracy:
I,Q components <+-1%

JPL

Pulse to pulse stability in test cavity (Michizono)

Digital feedback method

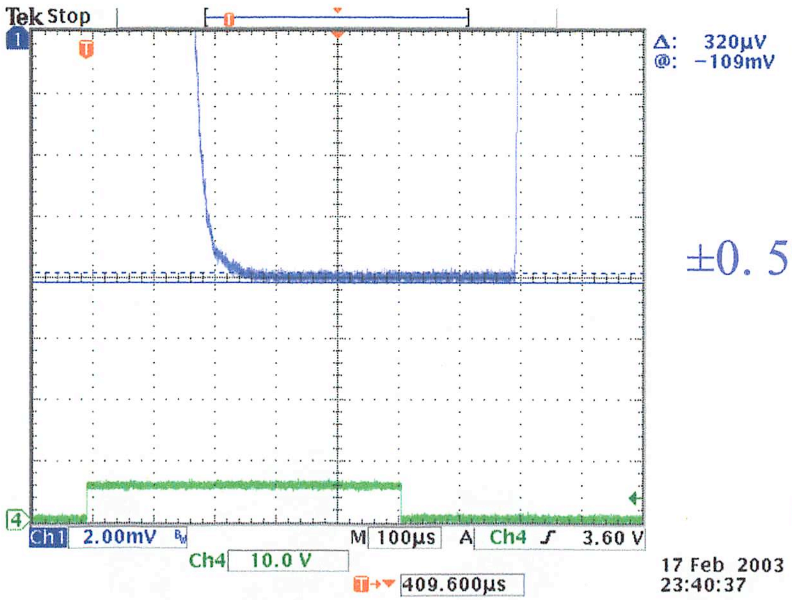

±0. 5%

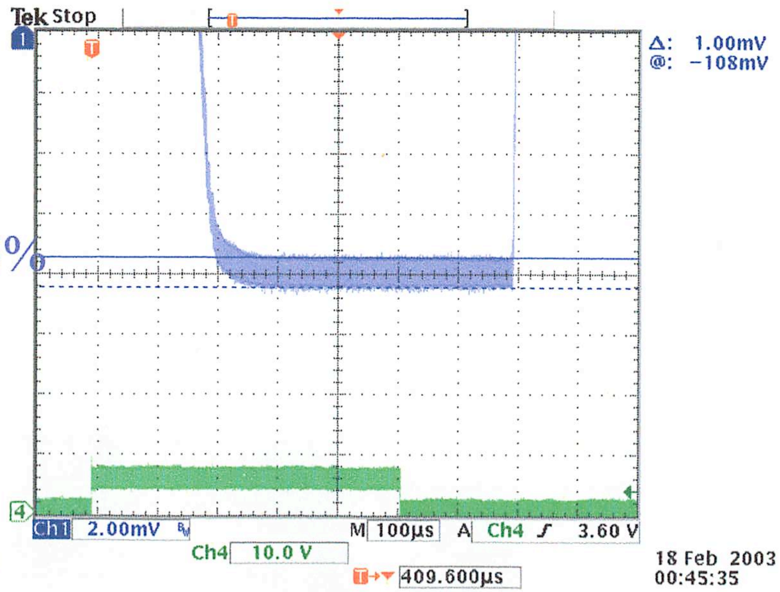

Single pulse

Envelope of ~150,000 pulses

The envelope signal (during 1hour 50pps operation) indicates the stability of less than +-0.3%.

Measurements of DT mechanical vibration

(Sakaki)

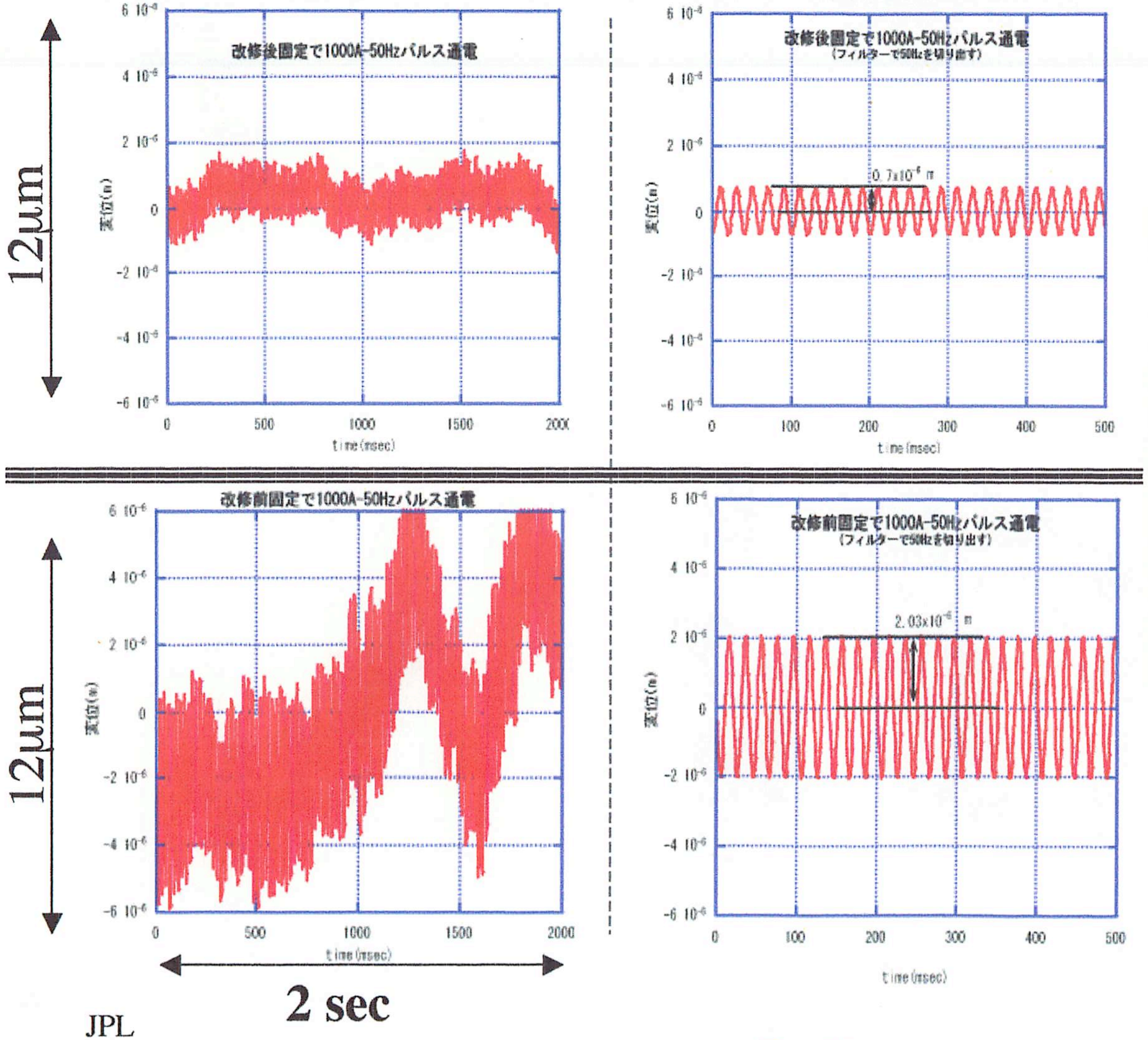

JPL

Displacement in the z-direction

50 Hz component

New data Feb. 2003

Peak ~ 0.7 µm at 50 Hz

No problem was found.
However,
Careful watching is necessary:
1) variation of resonant frequency,
2) if there were cooperative effects.

Old data before modifying the fixing method of DT stems.

Peak ~ 2 µm at 50 Hz

Chopper transient issues

- **Experimental results**
- **Calculated results using additional scrapers**
- **Future upgrade plan if required**
  - **Anti-chopper scheme**

Taking account of above three items, there is no serious problem in the transient chopped beam

Chopped beam measurements (June 2002)

experimental results (BPM signal at the exit of MEBT)

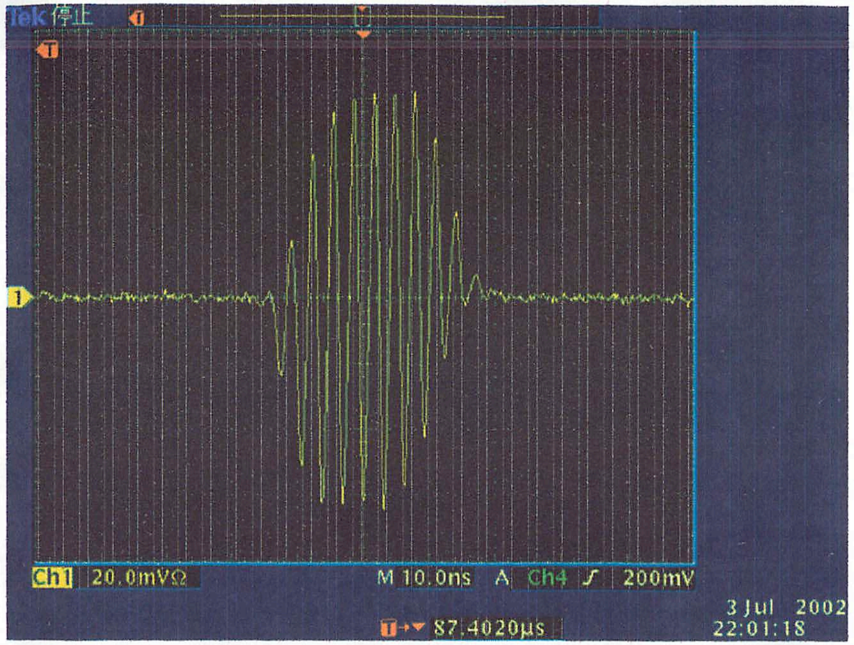

10 nsec/div

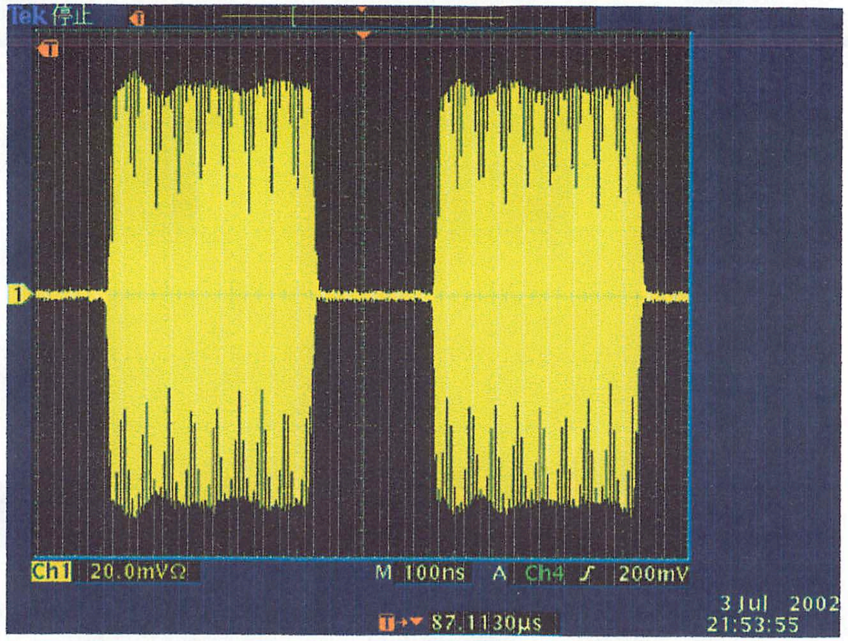

100 nsec/div

Transient rise/fall time ~10 nsec = 3 micro bunches.
No particles were observed at the MEBT exit during chopper on time up to 25 mA.
No effects due to chopper system were observed in the normal beam at the MEBT exit.

Transient deflecting field in the chopper

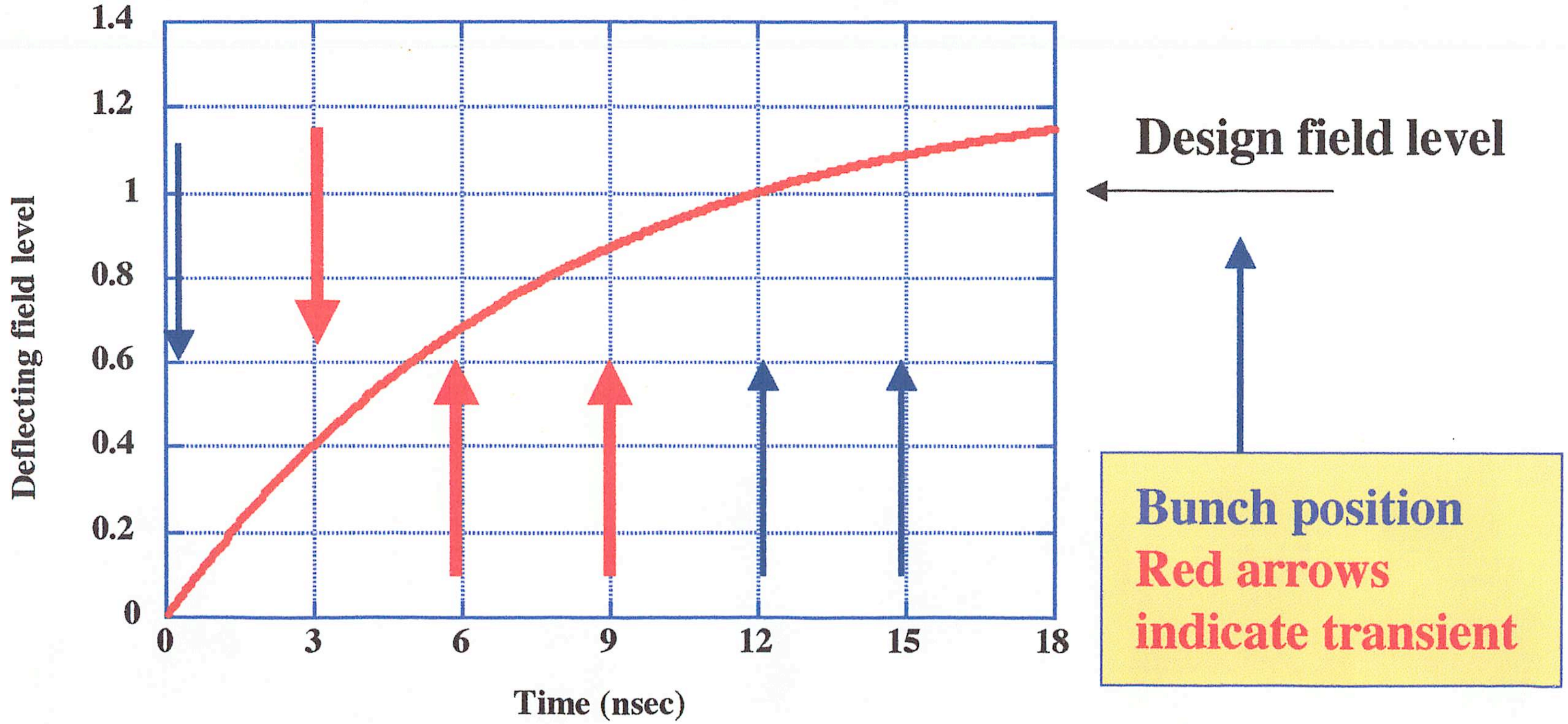

Relation between the field level and the transient time for the coupled RFD system. A fundamental period (bunch separation) is 3.08 nsec. Thus, position of micro-bunches during transient time influences total behavior.

Transmission ratio of the transient chopped particles along the linac-simulation results

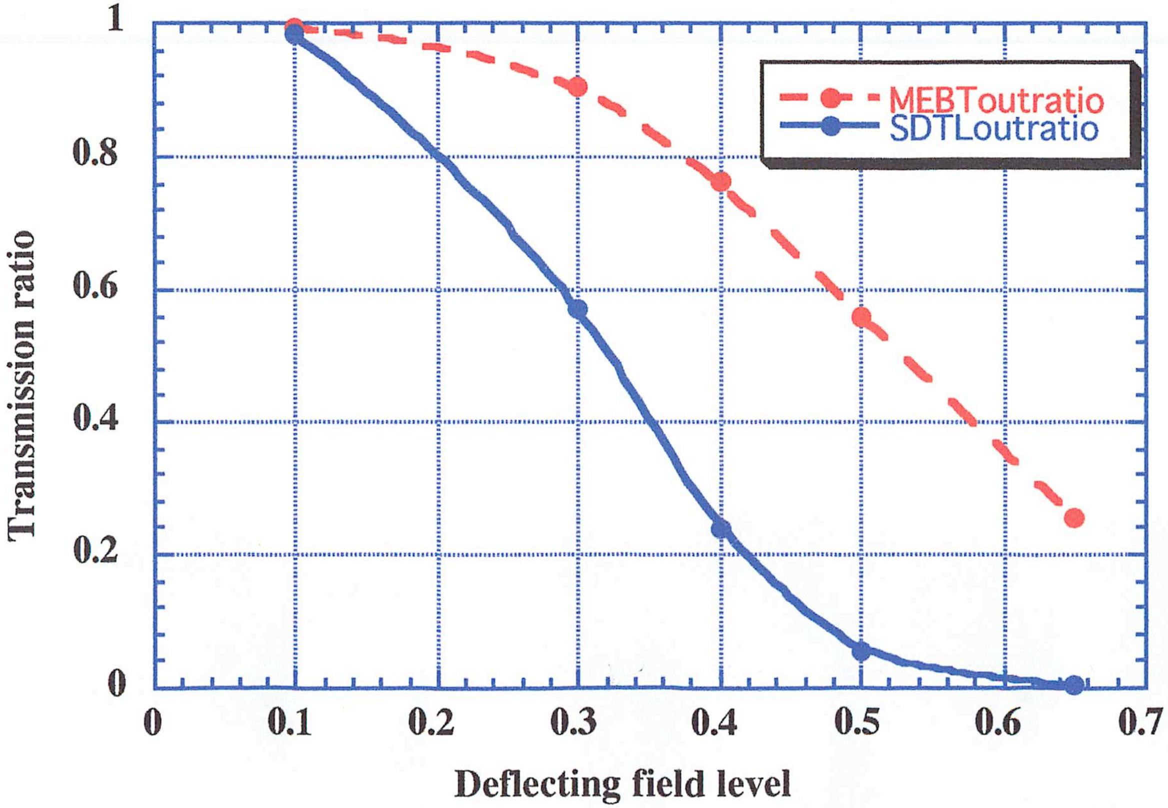

The calculation was done in 1997 at first. At that time, the output energy of the linac was 200 MeV.

Fig. 1 Transmission ratio of the transient chopped bunch through MEBT and SDTL vs. deflecting field. A scraper in the MEBT and two scrapers in the SDTL are assumed.

Transient chopped beam simulation

upto the SDTL

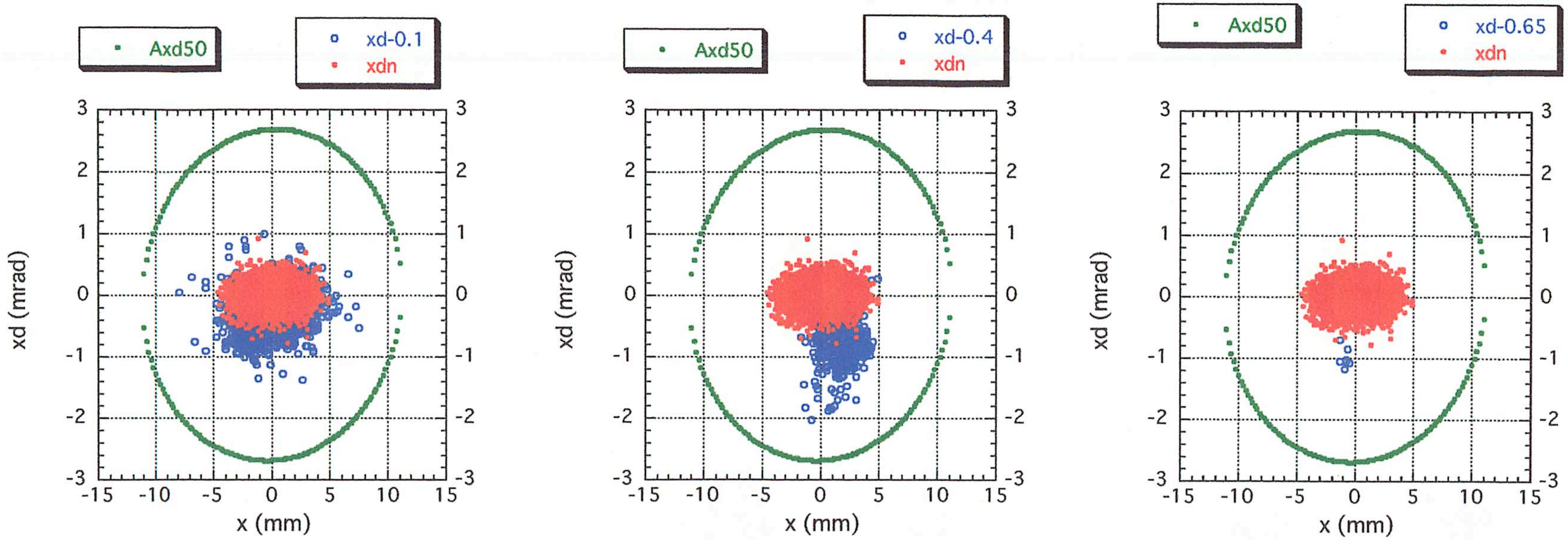

RFD field =0.1 **RFD field =0.4** **RFD field =0.65**

The emittances of the SDTL output beam. The large circle indicates half the SDTL acceptance (20π mm-mrad). Two kinds of the output were plotted in the same figure. The red filled circles corresponds to the normal bunch, while the blue empty circles indicate chopped bunch.

Ratio of the transient chopped bunch

- Total number of the transmitted transient chopped beam at the SDTL exit in terms of a bunch is 0.445 per one intermediate pulse.
- 0.17% of the incident beam into the MEBT at a 25 Hz and 500 μs operation.
- The equivalent beam power at 400 MeV is 420 W

Assumed deflecting field	0.41	0.65	0.87
Transmission ratio at DTL entrance	0.74	0.25	0
Transmission ratio at SDTL exit	0.22	0.0025	0

Anti-chopper scheme for improving transient behavior

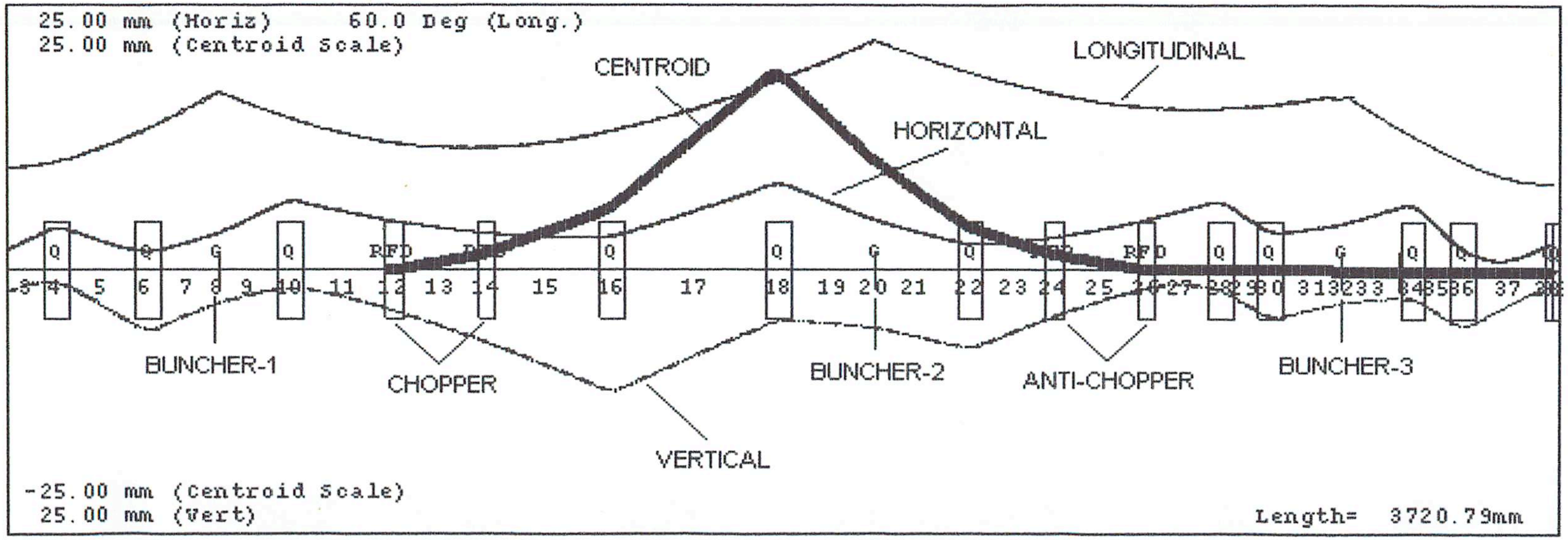

TRACE 3-D output of MEBT with an anti-chopper. The beam profiles in the z, x and y directions are shown. The coarse line traces the beam centroid deflected by two RF choppers and two RF anti-choppers. Another buncher and two choppers are required.

JPL

Details are in ref. LINAC-5.

Summary of transient chopped beam

1. If all transient particles (0.17%, 420W) are cut by the L3BT halo collimator system (limited to 4 π-mm-mrad), it can be allowed from the viewpoint of beam dump power (2 kW).
2. Main part of the transient beam arises from the bunch which is deflected by a deflecting field of around 0.4. In this case, the transient emittance and the normal one overlap partly. Therefore, some part of the transient beam passes through the L3BT halo system and reaches to the RCS. It is no problem, since the emittance is smaller than 4 π -mm-mrad.
3. The estimated transverse acceptance of the ACS is about 70 π -mm-mrad (100%). Therefore, I think that the acceptance of the ACS is sufficiently large for accelerating the transient chopped beam.
4. It was shown that the timing of the transient micro-bunch related to the start time of the deflecting field is very important, since the field level for the transient chopped beam determines its transmission behavior along the linac.
5. Anti-chopper method will be used if necessary.

End-to-end simulation including errors

- Modified PARMILA simulation in 1999
  - RFQ-DTL-SDTL-ACS
  - Including field errors, Q-magnet position errors
- LINSAC simulation
  - MEBT-DTL-SDTL-ACS-L3BTarc2
  - Including field errors, Q-magnet position errors

Modified PARMILA simulation in 1999

- **RFQ-DTL-SDTL-ACS simulation (25000 particles)**
- **Two kinds of input particles**
  - **Generated beam (C-type)**
  - **RFQ output beam (RFQ-type)**
- **Including errors both in transverse and longitudinal**
  - **Error - 1**
    - **±1% cell and tank fileds**
    - **±1% cell phase and ±3% tank phase**
    - **Q-magnet displacement ±0.05 mm**
  - **Error - 2**
    - **±2% cell and tank fields**
    - **±2% cell and ±6% tank phase**
    - **Q-magnet displacement ±0.1 mm**
- **Three kinds of injection matching method**
  - **Matched beam parameters by calculation**
  - **Rms matching by test simulation**
  - **Minimizing rms or 99.9% emittance growth by test simulation**

Input beams

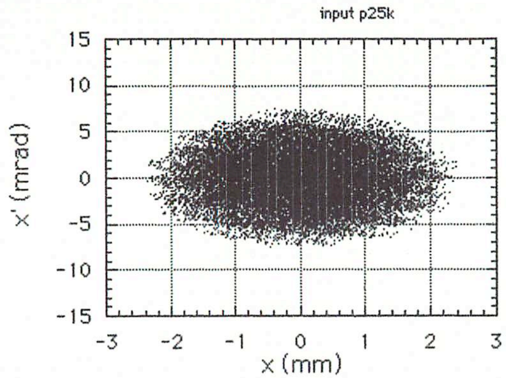

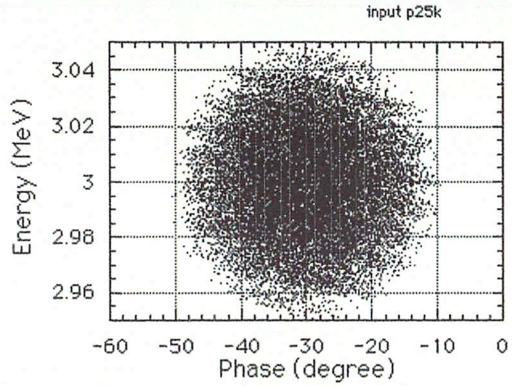

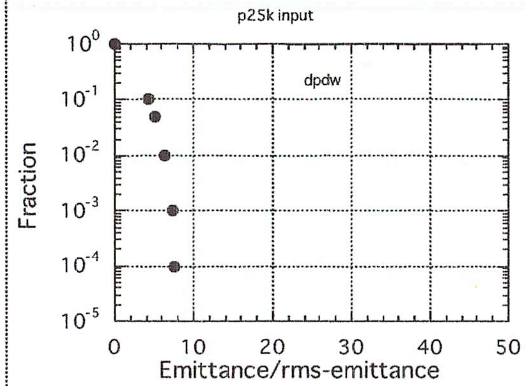

C-type

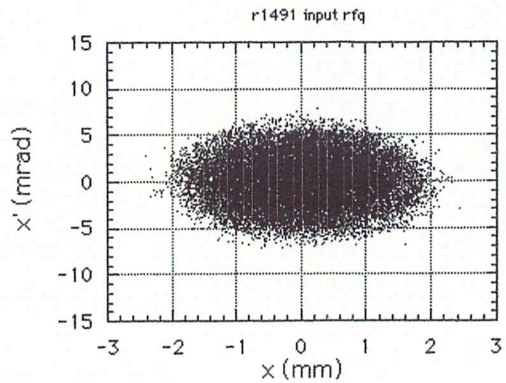

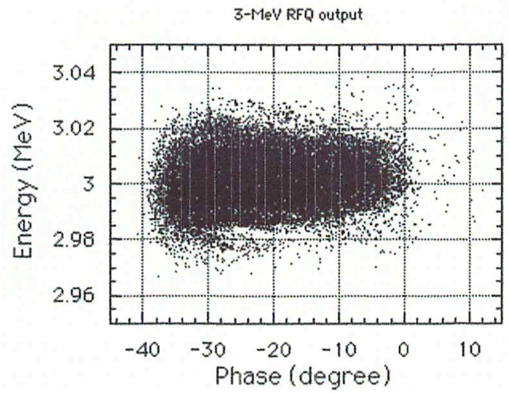

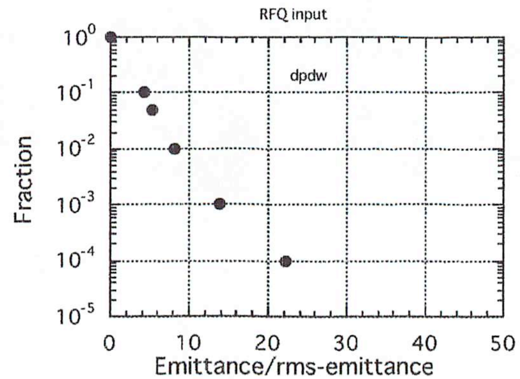

RFQ

ΔφΔw Beam fraction

ACS output beams (Type-1 error)

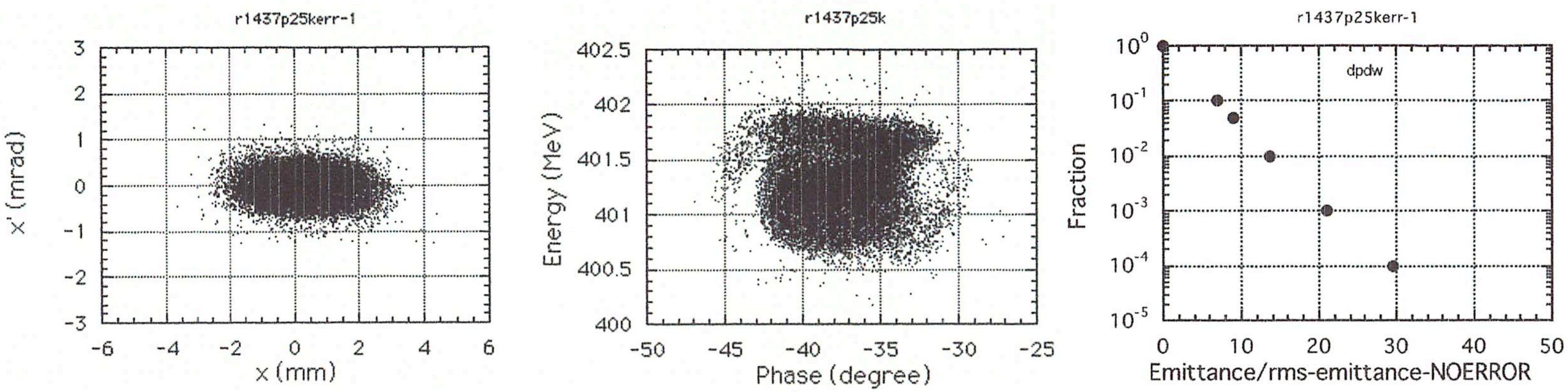

C-type

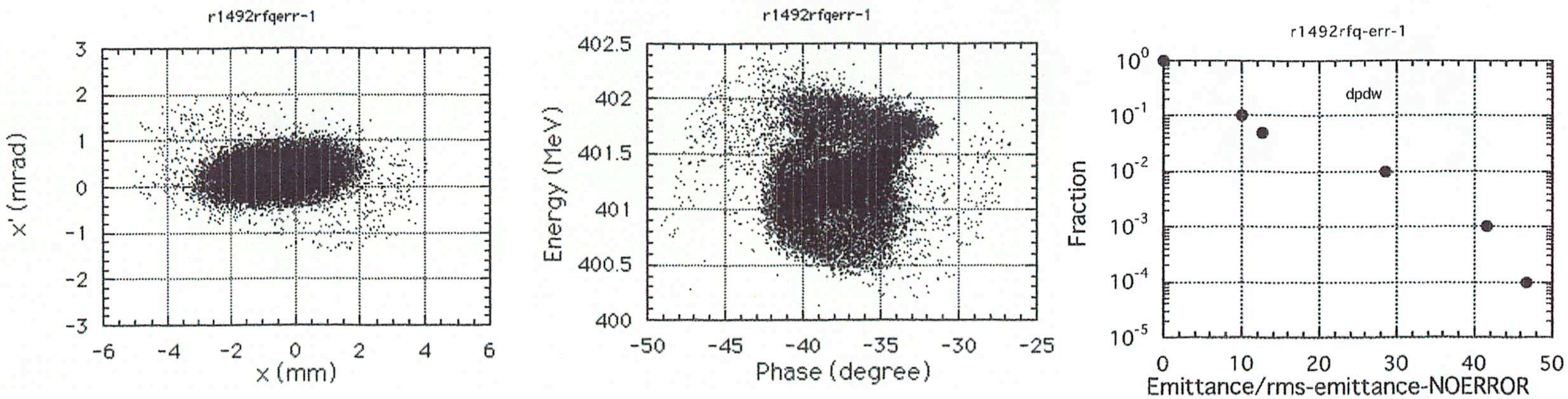

RFQ

JPL

ΔWmax < ± 1.25 MeV

ΔφΔw Beam fraction

Emittance variation (Type-1 error, PARMILA)

C-type injection beam

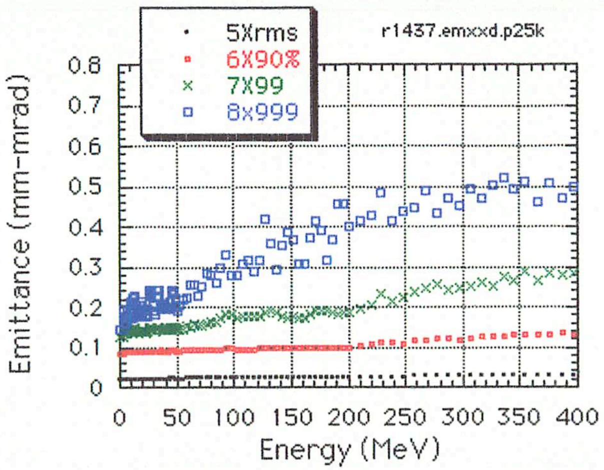

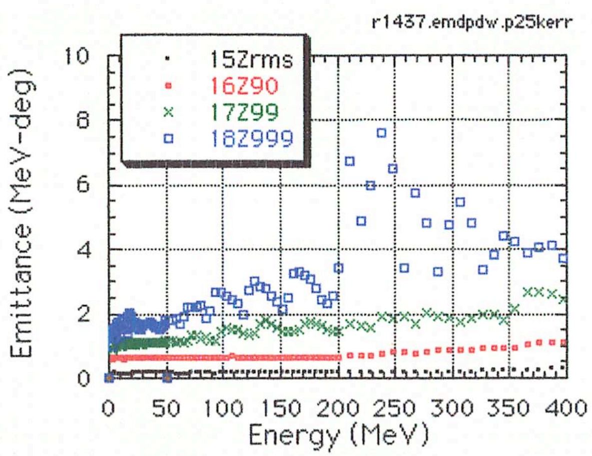

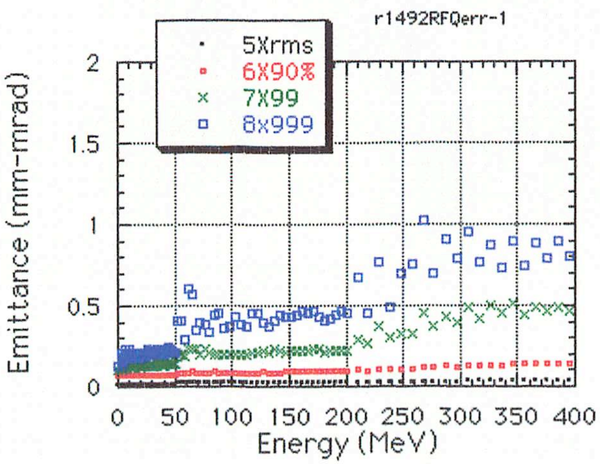

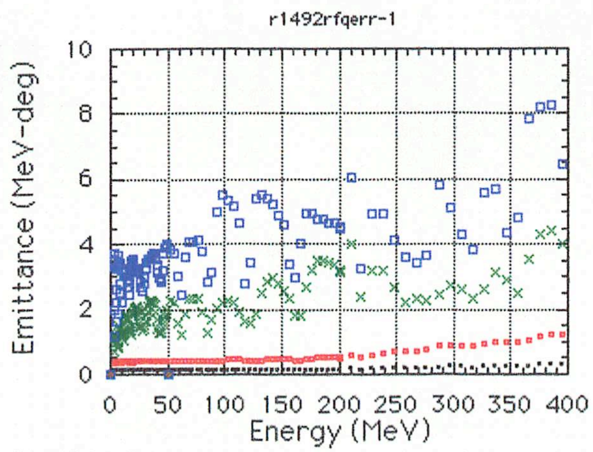

RFQ injection beam

Summary of output emittance (PARMILA)

x-x', π-mm-mrad

	C-input	C-err-1	C-err-2	rfq-in	rfq-err-1	rfq-err-2
rms	0.198	0.299	0.628	0.164	0.339	0.687
90%	0.842	1.32	2.83	0.703	1.45	3.06
99%	1.25	2.81	8.26	1.08	5.11	9.50
99.9%	1.44	4.97	20.6	1.33	10.6	18.3

y-y', π-mm-mrad

	C-input	C-err-1	C-err-2	rfq-in	rfq-err-1	rfq-err-2
rms	0.198	0.326	0.626	0.161	0.371	0.805
90%	0.847	1.48	2.71	0.693	1.66	3.44
99%	1.24	2.55	7.34	1.06	3.91	11.4
99.9%	1.42	5.01	13.7	1.32	10.2	20.2

ΔφΔW, π-MeV-deg

	C -err-1	C -err-2	rfq-err-1	rfq-err-2
rms	0.793	3.23	0.871	3.60
90%	3.44	8.77	3.74	10.3
99%	6.80	19.2	10.7	25.7
99.9%	10.4	66.1	15.6	75.5

Details are in ref. LINAC-4.

Type-2 error simulation (PARMILA)

- Some beam losses are observed in the error-2 simulation
  - **C-type: 0.1% beam losses**
  - **RFQ: 0.04% beam losses**
- **Thus, Type-2 error is not acceptable.**

±2% cell and tank fields
±2% cell and ±6% tank phase
Q-magnet displacement ±0.1 mm

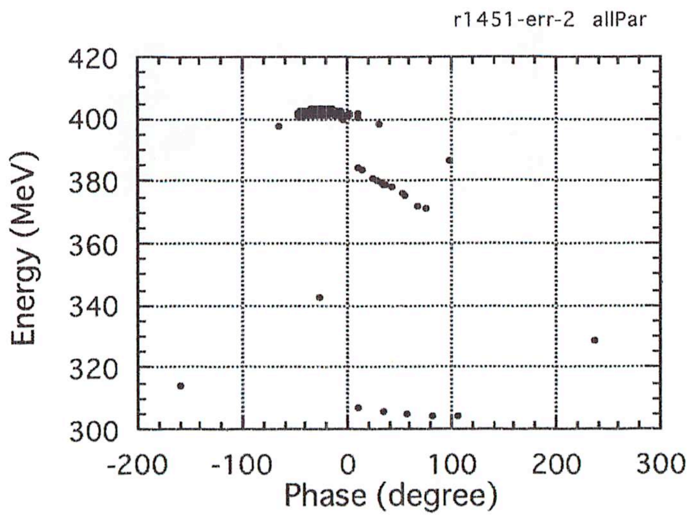

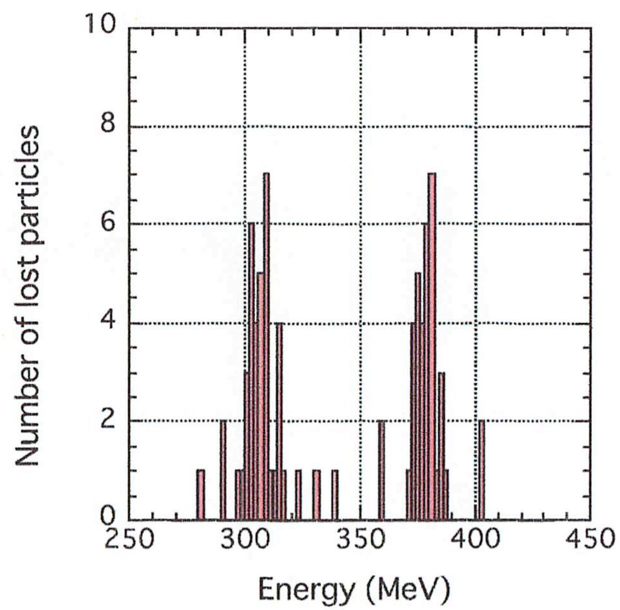

Effects of error distribution (longitudinal)

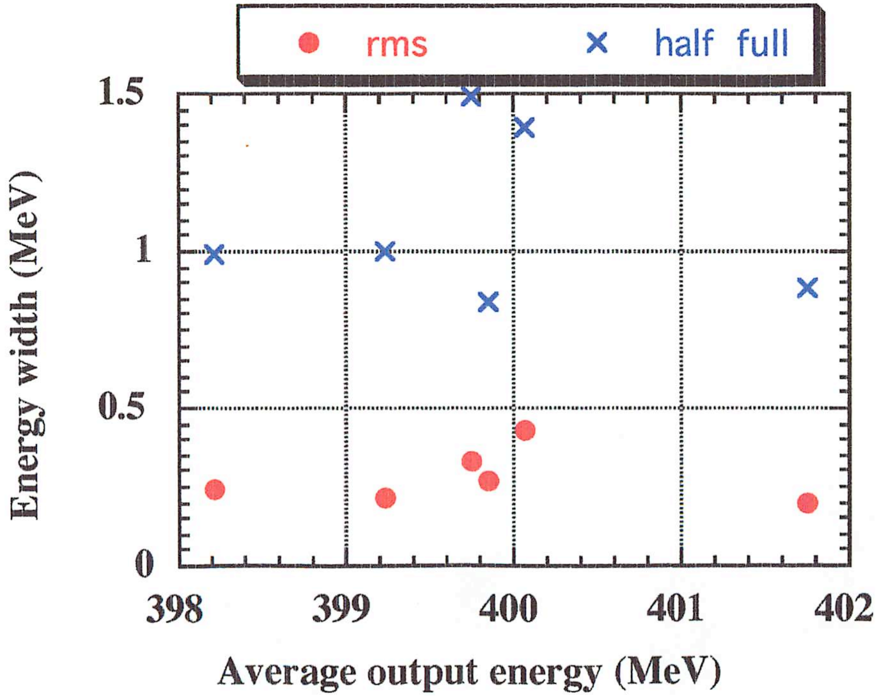

1) Accelerating field errors: ±1%, 1 degree for DTL, SDTL, ACS.
2) Q-magnet: Δx, Δy ±50μm.
3) Change longitudinal error distribution in ACS.

Waverage < ±2 MeV
Δw (half full) < 1.5 MeV

If the error is static, the effects can be compensated along the linac.

Energy deviation of the 400-MeV linac

Deviation of the output energy from the design value versus the maximum energy-oscillation amplitude in the structure for sixty random-error simulations.

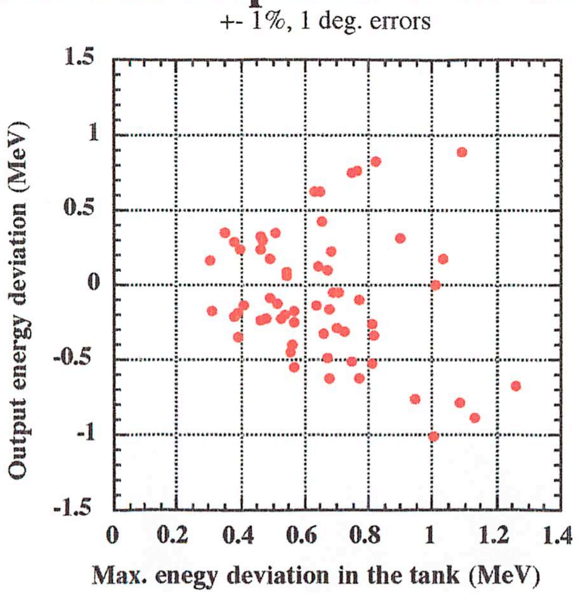

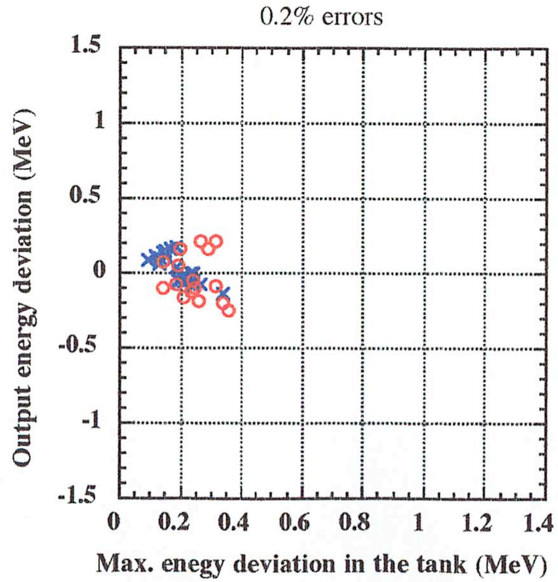

Amplitude error: two kinds of cell-error distribution of ±1%, varied tank error of ±1%.
Phase error: two kinds of cell-error distribution of ±1degree, varied tank error of ±1 degree.

Amplitude error: two kinds of cell-error distribution of ±1%, varied tank error of ±0.2%.
Phase error: two kinds of cell-error distribution of ±1degree, varied tank error of ±0.2 degree.

Debuncher operation (1)

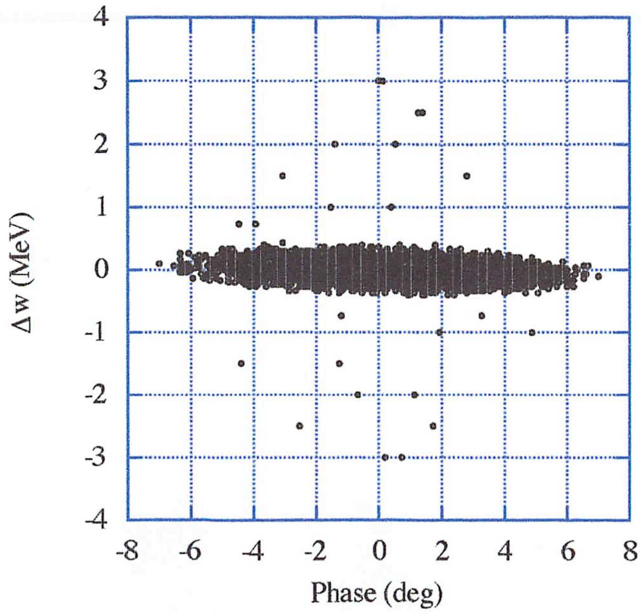

ACS output + artificial halo-particles at the ACS exit.

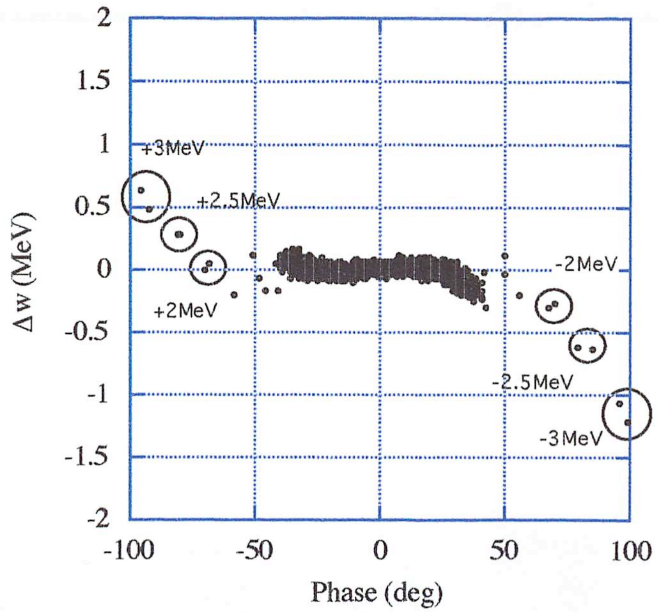

After debuncher

Energy width of ± 2 ~ 2.5 MeV is acceptable

Debuncher operation (2)

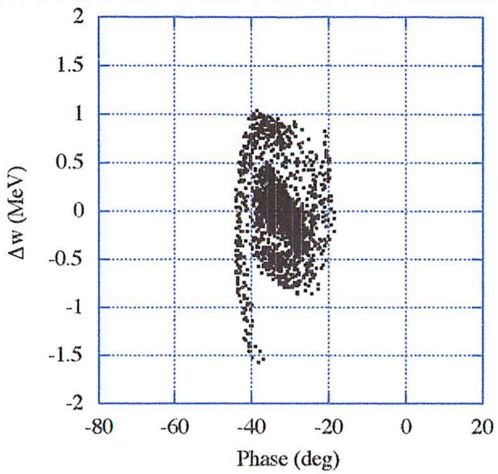

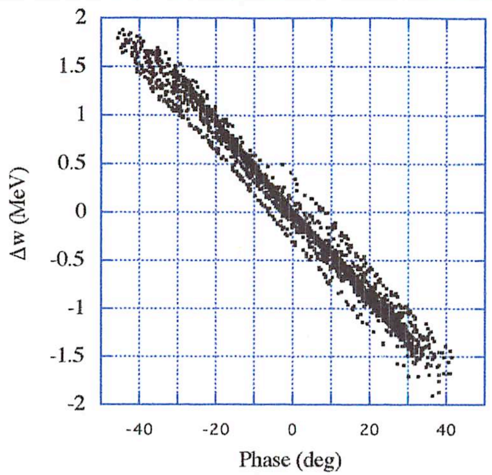

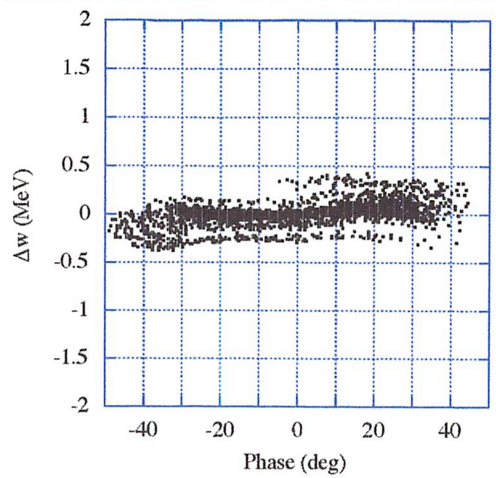

Example of bad ACS output emittance.
Tank: $\Delta\phi = \pm 1$deg,
$\Delta Ez = \pm 2\%$,
$\Delta\phi$_injection= +5 deg.

Just before debuncher.

After debuncher

JPL

Conclusion: output energy width

- **Stability of RF field amplitude < +- 0.3%**
- **Stability of RF phase < +- 0.2 degrees**
- **Debuncher operation**

Experimental results satisfy the requirement with a sufficient margin.

The requirement of $\Delta p/p < 0.1\%$ can be achieved without longitudinal collimation system in L3BT.

(Here, short-time stability is considered)

MEBT simulation results

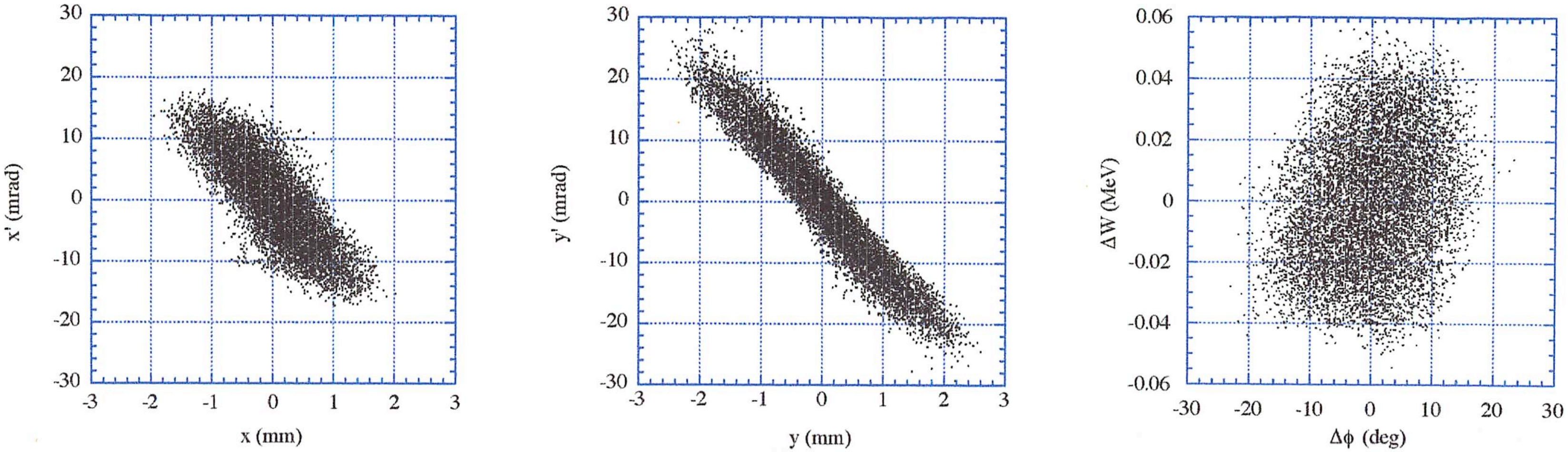

	Rms	90%	99%	π-mm-mrad, 9600 粒子
ε_x in	0. 198	0. 806	1. 06	
ε_x out	0. 222	0. 947	1. 73	
ε_y in	0. 201	0. 818	1. 08	
ε_y out	0. 233	0. 997	1. 84	

MEBT simulation -summary

- Rms transverse emittance growth of 10 - 15% roughly agrees with the experimental results
- Large growth in 99% emittance
- The above results are allowed from the viewpoint of final output beam emittance in the LINSAC simulation
- Simulations using the calculated RFQ beam were performed in 1999

LINSAC simulation (400 MeV)

- 3200 & 9600 particles
  - No error
  - Type-1 random errors
    - Field amplitude ±1%, phase ± 1 deg., deviation of the Q-magnet position ±0.05 mm
  - Type-2 random errors
    - Field amplitude ±1%, phase ± 1 deg., deviation of the Q-magnet position ±0.1 mm
  - MEBT - DTL - SDTL - ACS - arc2 of L3BT

(Type-2 error in PARMILA simulation and that in LINSAC is different)

Emittance variation along the linac

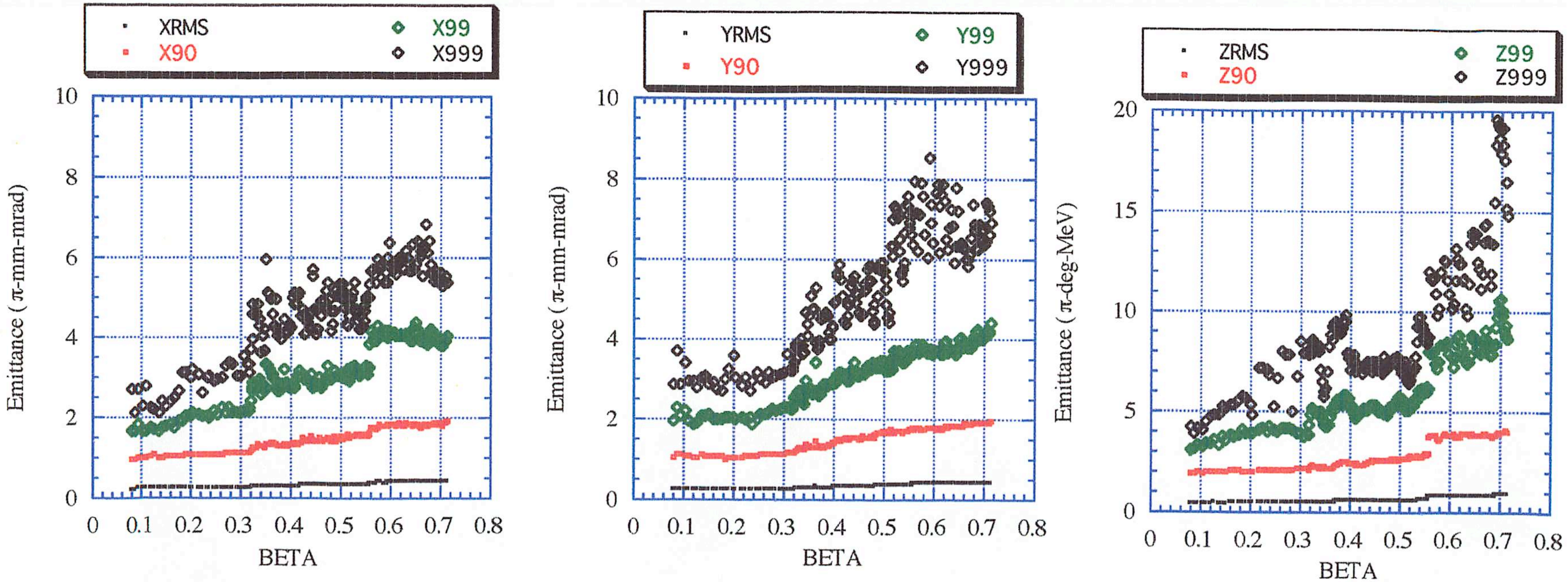

Type-1 errors: 3200p, MEBT-DTL-SDTL-MEBT2-ACS

Some improvements are planned: tuning in the MEBT2, tuning of the matching of the transition parts, modification of the buncher part of LINSAC code.

Summary of ACS output emittances (LINSAC)

	π-mm-mrad						π-MeV-deg			MeV	MeV
	xrms	x90	x99	yrms	y90	y99	zrms	z90	z99	dw_{rms}	dw_{max}
INPUT	0.199	0.814	1.06	0.201	0.816	1.09					
3200 particles											
a107 no-error	0.371	1.63	3.35	0.390	1.71	4.10	0.874	3.80	8.81	0.258	1.18
b108 error-1	0.416	1.93	4.03	0.434	1.95	4.40	1.01	4.42	9.52	0.427	1.39
b113 error-2	0.500	2.28	4.74	0.522	2.41	5.12	1.28	5.57	14.8	0.314	1.35
9600 particles											
a109 no-error	0.391	1.75	3.86	0.388	1.72	3.81	0.886	3.89	9.07	0.258	1.17

Error-1: ±1%, ± 1deg, ±0.05 mm   Error-2: ±1%, ± 1deg, ±0.1 mm

L3BT simulation (LINSAC)

- **ACS output beam was injected into L3BT**
- **Up to the arc-2 for three kinds of Q-magnet position errors: no error, ± 0.05 mm and ± 0.1 mm**

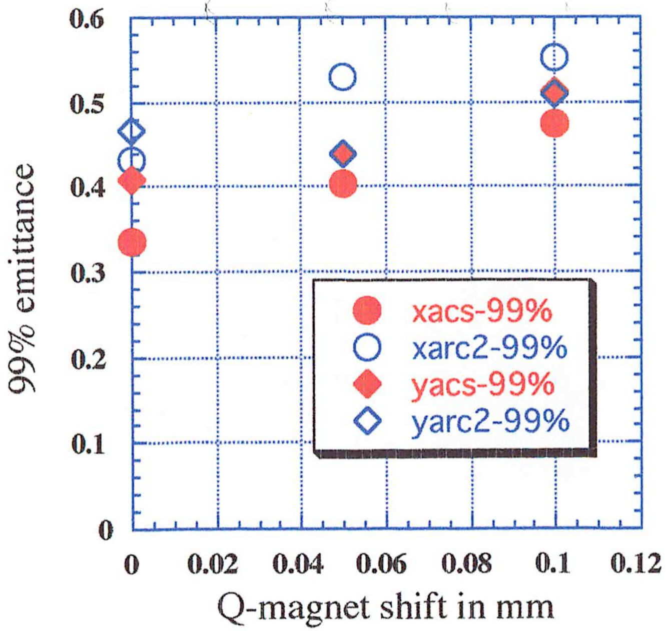

99% emittances at the entrance of L3BT and the exit of the arc-2.

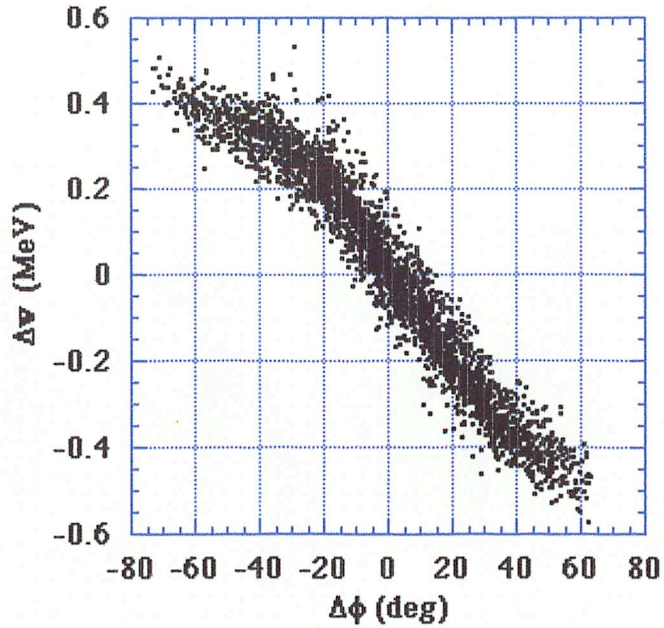

ΔφΔW emittance at the exit of arc-2

Simulation codes for JPL (plan, near future)

Availability of input files:

	MEBT1	DTL	SDTL
PARMILA	Ready	Preparing	Ready
IMPACT	Ready	Preparing	Ready
LINSAC	Ready	Ready	Ready

	MEBT2	ACS	L3BT
PARMILA	Ready	Ready	Ready
IMPACT	Ready	Ready	
LINSAC	Ready	Ready	Ready

Further detailed and systematic simulation studies are planned after designing urgent issues for construction.

L3BT new design

- Suppress strong space-charge effects with an equivalent 150 mA beam
- Suppress emittance growth along the L3BT
- Tuning-free arc-1 for a varied peak current
- Satisfy requirements from RCS injection

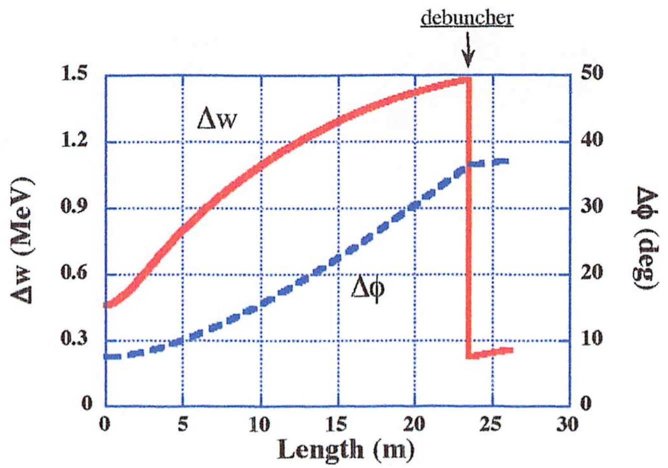

$$\frac{\sigma}{\sigma_{0x}} = 0.6 \sim 0.7$$

Longitudinal behavior in the beginning part of the L3BT.

Solution

- **No use of longitudinal collimation system**
  - **Not necessary, judging from estimation of Wave, ΔW and acceptable energy range of debuncher operation**
  - **Avoid undesirable effects due to combination of large dispersion, large beam size and the strong space-charge effects, arising from the arc section**
- **Use Double Bend Acromatic lattice for 90-degree Arc section**
  - **Use sufficient focusing strength,**
  - **Avoid effects due to large dispersion combined with the space-charge effects**
  - **Tuning free from change of peak current**

L3BT layout

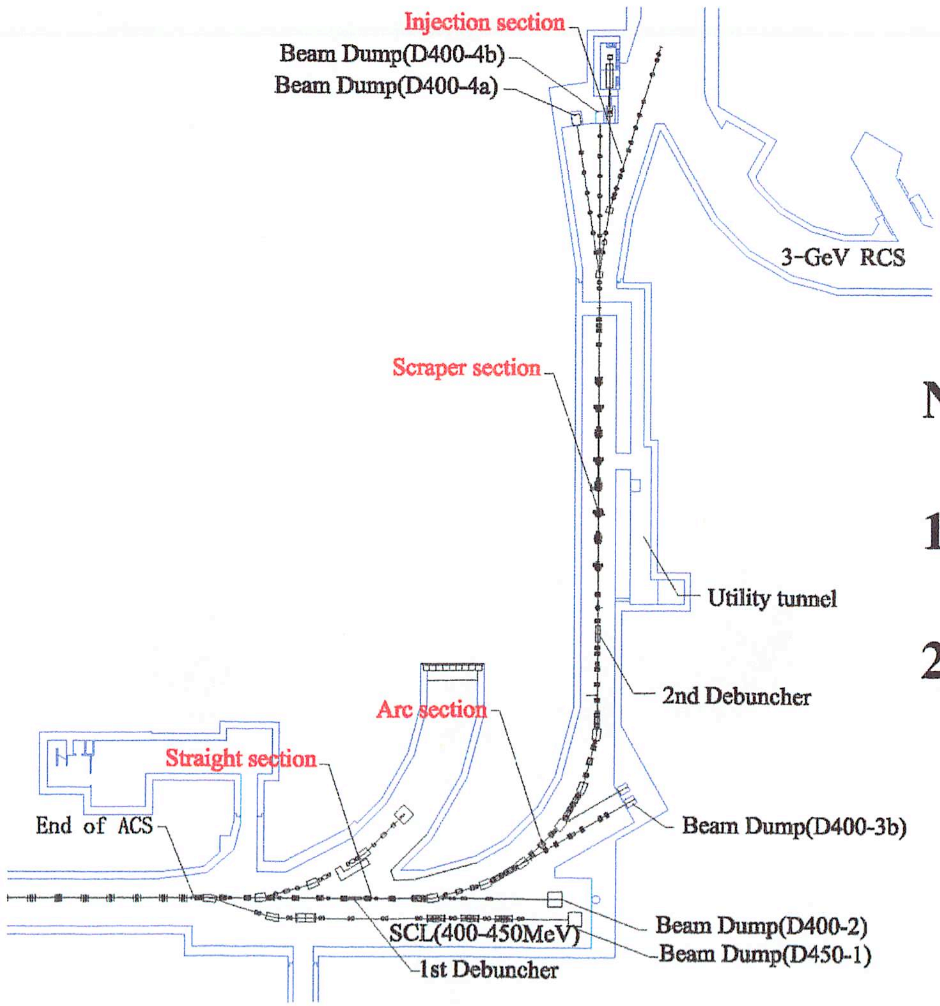

NEW DESIGN FEATURES:

1. **No longitudinal collimation system**
2. **Double bend acromatic lattice for the first 90 deg. arc.**

L3BT lattice

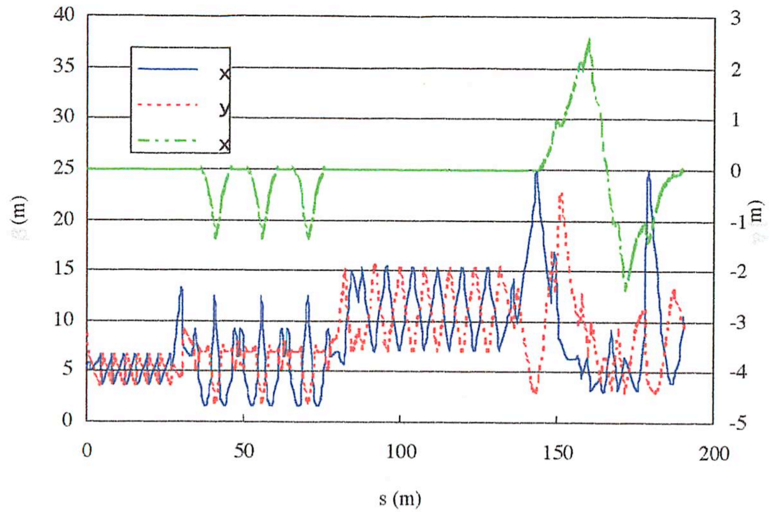

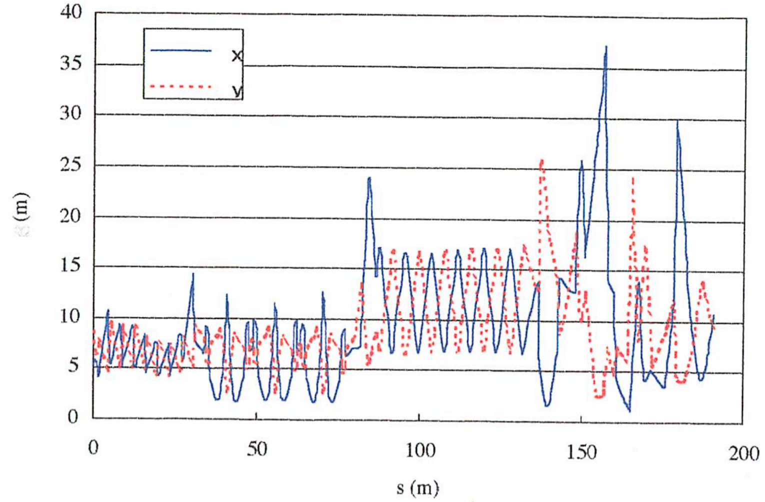

β-functions (both x and y directions) and η-function of the L3BT (0 mA).

150 mA

JPL

Double Bend Acromatic lattice (DBA) for arc-1

β and η functions

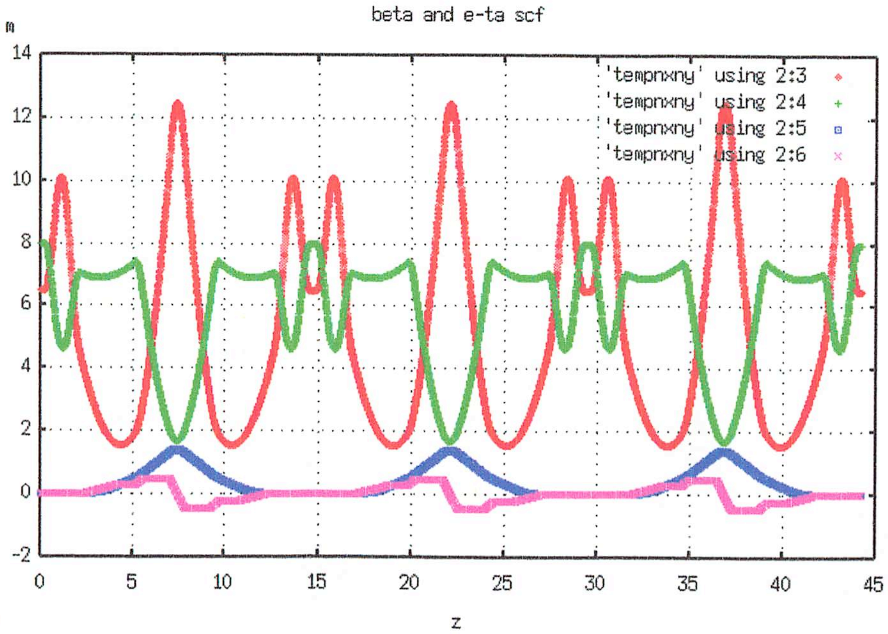

0 mA, after tuning

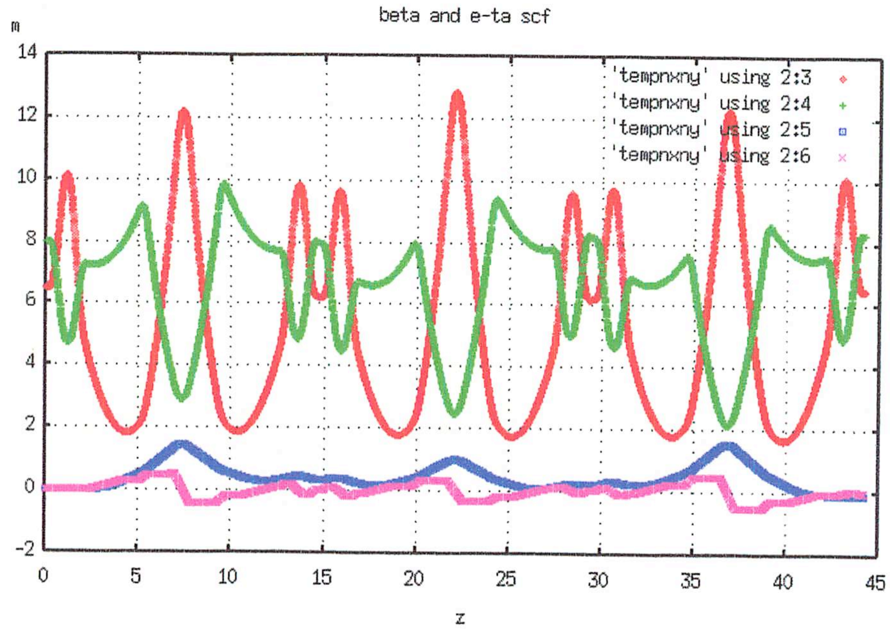

150 mA, the same tuning for 0 mA beam

A change in the beam parameters due to variation of the peak current is small.

JPL

PARMILA simulation results (Matsuoka)

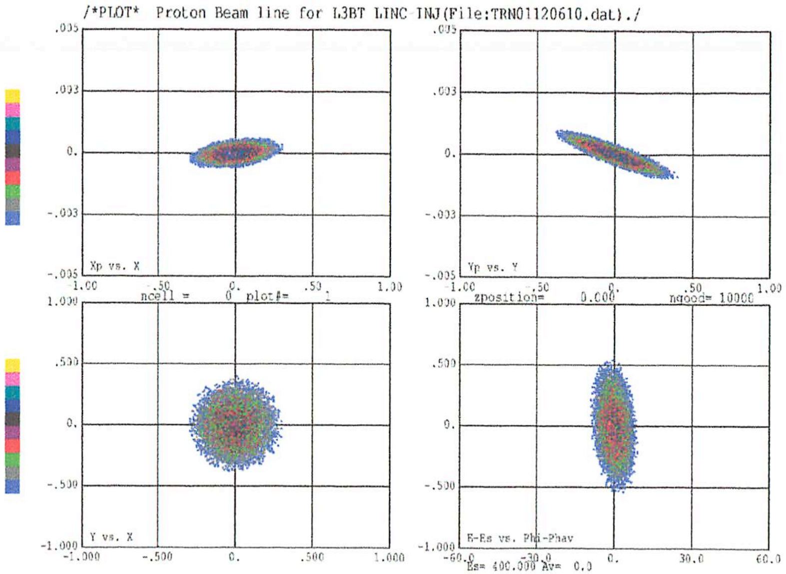

Input beam to L3BT.

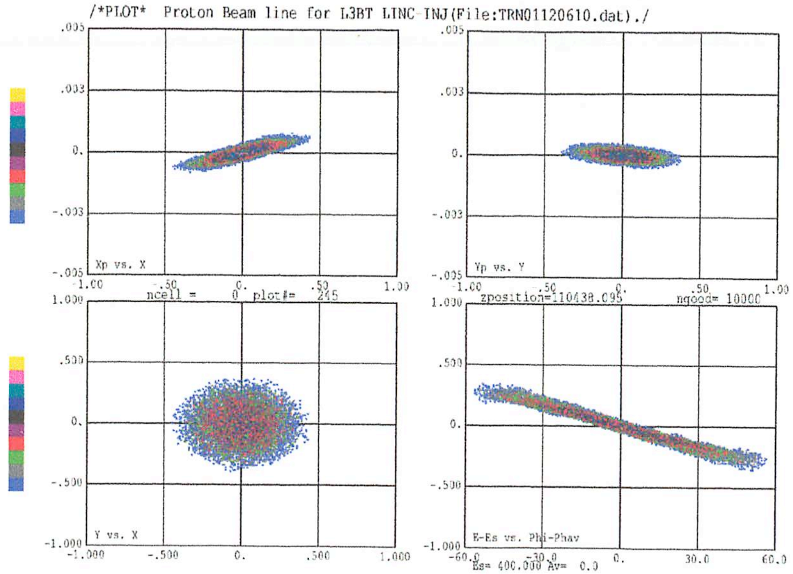

Output beam from L3BT

Table 2-1-5-1 Beam parameters at the injection point.

	Simulation result	Requirement
Transverse emittance (99.9%)		
Horizontal	1.8 π*mm*mrad	4 π *mm*mrad
Vertical	1.9 π *mm*mrad	4 π *mm*mrad
Momentum spread	±0.078%	±0.1%

Summary

- Basic design principles are explained.
- Progress in construction and simulation is summarized from the viewpoint of stability and errors.
- Transient chopped beam issues and analysis are reported.
- Multi-particle simulation studies are summarized.
- L3BT new design is presented.